Title
Mid-infrared reflectivity of experimental atheromas

Authors
Holman, Hoi-Ying N.
Bjornstad, Kathy A.
Martin, Michael C.
et al.

Publication Date
2008-06-30

Mid-Infrared Reflectivity of Experimental Atheromas

Hoi-Ying N. Holman, Ph.D.[1*], Kathy A. Bjornstad, B.A. [1], Michael C. Martin, Ph.D.[1], Wayne R. Mckinney, Ph.D[1]., Eleanor A. Blakely, Ph.D.[1], and Francis G. Blankenberg, M.D.[2*]

[1] Lawrence Berkeley National Laboratory, University of California, Berkeley, CA 94720, USA.

[2] Division of Pediatric Radiology/Department of Radiology, Stanford University Hospital, Stanford, CA 94305, USA.

[*] Communicating Authors:

Francis G. Blankenberg, M.D.

Division of Pediatric Radiology/Department of Radiology, Stanford University Hospital

725 Welch Road, Rm #1673, Lucile Packard Children's Hospital, Stanford, CA 94305

Phone: (650) 497-8601

Fax: (650) 497-8745

e-mail: blankenb@stanford.edu

Hoi-Ying N. Holman, Ph.D.

Mailstop: 70A-3317L, Lawrence Berkeley National Laboratory

One Cyclotron Road, Berkeley, CA 94720

Phone: (510) 486-5943

Fax: (510) 486-7152

e-mail: hyholman@lbl.gov

Abstract

Here we report that the pathologic components present within the atheromatous plaques of ApoE knock-out mice can reflect significant amounts of mid-infrared light. Furthermore, the reflected light spectra contained the unique signatures of a variety of biologic features including those found in unstable or “vulnerable” plaque. This discovery may represent a unique opportunity to develop a new intravascular diagnostic modality which can detect and characterize sites of atherosclerosis.

Vulnerable plaques (VPs) are metabolically active and histologically complex atheromas with thin fibrous caps that are prone to spontaneous rupture often leading to sudden death.[1] Direct angiography, the most widely used method to evaluate the coronary vessels, cannot distinguish between a VP and a less metabolically active stable plaque. For decades, mid-infrared spectroscopy has been used to characterize the pathologic biochemical changes within thin sections of atheromas including vulnerable plaques (VPs) ex vivo.[2-5] A variety of absorption peaks and bands within the mid-IR transmission spectra have been specifically linked to the vibrations of atoms within functional groups of many characteristic molecules that compose an atherosclerotic lesion, such as atherogenic lipoproteins, phospholipid particles, cholesterol ester and fatty acids. Unfortunately the high native water content within the arterial wall and its strong interfering absorption has severely limited the use of mid-infrared spectroscopy as in vivo imaging modality for atherosclerosis.

There are however, alternative ways to use infrared light to interrogate tissue samples that can circumvent these difficulties, including spectral analyses of the absorption patterns from "reflected" as opposed to "transmitted" infrared light, coupled to a bright but harmless light emitter such as a synchrotron.[6] In this article we describe how mid-infrared light is reflected by pathologic components in the diseased aortic intima of ApoE (-/-) mice. Furthermore, the reflected light contains the spectral signatures of pathologic molecules associated with atheromas including VPs.

Reflection-based mid-infrared spectroscopy is a well-established technique (see reference #7). Because of the unique contrast mechanism associated with this technique, it has been widely used for the characterization and structure-property elucidation of multilayered materials.[7] We

have previously extended this technique to measure the reflection-absorption Fourier transform infrared spectra (FTIR) of microbial communities located on geological materials that contain multiple reflective interfaces of different optical properties.[6] We postulated that this spectroscopic technique could also be applied to whole tissues in which a subsurface change in refractive index in effect creates a reflective interface among the pathologic molecules of interest. This type of interface exists within the intima of atherosclerotic vessels where non-native lipid (with an average refractive index of 1.45 to 1.50, depending on the composition and sizes of lipid particles[8]) and calcium deposits like hydroxylapatite or calciumphosphate (with an average refractive index of at least 1.63[9]) are found in great abundance. In contrast, normal intimal tissues are ~80% water content, relatively uniform in optical properties, and generally have an average refractive index of approximately 1.35 – 1.38 (by extrapolation from literature).[10, 11] Although these refractive indices are for the visible regime, as a first estimation, they could mirror the differences within the complex atherosclerotic matrix.

Conceptually, mid-infrared light that enters an atheroma would encounter multiple refractive boundaries, wherein some light might be reflected and re-emerge under certain conditions. From first principles, if the surface roughness at the refractive boundary is larger than the wavelength of the incoming light, the light that is not absorbed would undergo multiple diffuse reflections before re-emerging. If the surface roughness is smaller than the wavelength (i.e., the surface is nearly smooth), unabsorbed light can experience a quasi-specular reflection before re-emerging. The lack of accurate information on the wavelength-dependent refractive index, absorption coefficients and the surface roughness of atherosclerotic interfaces makes it difficult to numerically predict the detectable reflectivity. Given the morphologic complexity of most atheromas, the final detectable signal would likely be the sum of these two modes of

reflectivity. It is also likely that, the features of the reflected infrared spectra would contain the absorption patterns generated by the major pathologic components of an atheroma, namely; atherogenic lipoproteins, extracellular phospholipid particles, smooth muscle cells, foam cells, and disintegrating foam cells as they undergo apoptotic cell death.[12, 13]

To test if such reflectivity exists, we made infrared measurements on the explanted aorta of a 9 month old female adult ApoE (-/-) mouse fed a high-fat diet. ApoE (-/-) mice [i.e. homozygous for the *Apoe*^{tm1Unc} mutation] (C57BL/6 x 129SvJ) and wild-type controls were obtained from Jackson Laboratories (Bar Harbor, Me). ApoE (-/-) mice were placed on a high fat/cholesterol (1-2%) diet for 3 months until sacrifice. We employed Beamline 1.4.3 at the Advanced Light Source (ALS) synchrotron at LBNL (http://infrared.als.lbl.gov/) as our mid-infrared source. The synchrotron infrared beam has brightness in the range of approximately 10^{11} to 7×10^{12} photons/sec-mm^2 mrad-0.1%BW when focused to a 10-micron spot. Each aortic specimen was placed luminal side up beneath an infrared-transparent ZnSe window (International Crystal Labs, NJ) inside a custom-built environmental chamber where the temperature was kept at ~5°C to maintain the "freshness" of the specimens during reflectivity measurements. All FTIR measurements were recorded in the standard reflection mode in the mid-infrared 4,000 to 650 cm^{-1} region, and consisted of 128 co-added spectra at a spectral resolution of 4 cm^{-1}.

Fig. 1 shows examples of the FTIR measurements collected along a cluster of different types of atheromas including histologically advanced lesions (VPs; confirmed later by routine histologic examination) within the aortic arch. A significant number of mid-infrared photons (Fig. 1a) that entered any given atheroma were reflected and emerged from the tissue sample (Fig. 1b). In contrast, few were reflected from the non-diseased portions of aorta (Fig. 1c). A

striking feature was that the reflected light contained the spectral features (Fig. 1d) known to be associated with atherosclerotic disease.[3-5] For instance, the 3100 to 2800 cm^{-1} region revealed similar spectral features known to arise from the carbon hydrogen bond stretching vibrations of fatty acids and cholesterol esters, including the –HC=CH– moiety of their unsaturated hydrocarbon chains at ~3010 cm^{-1}, or from their acyl CH_2 groups at ~2925 and ~2852 cm^{-1}.[3, 4] The strong absorption at ~1745 cm^{-1} also matched the spectral profile of the C=O stretching vibrations of ester carbonyl (>C=O) groups that are found in atherogenic phospholipid. The broader absorptions in the 1700 to 1500 cm^{-1} region had comparable features to those generated by the >C=O stretching of the amide I and of the N–H bending of the amide II modes present in the peptide groups of proteins. In the 1500 – 1000 cm^{-1} fingerprint region, absorption characteristics at ~1465 and ~1375 cm^{-1} were similar in nature to the vibrations of the lipid acyl CH_2 and to the symmetric bending of the lipid methyl CH_3 groups, respectively. The absorptions at ~1240 and ~1090 cm^{-1} matched the spectral patterns known to arise from the asymmetric and symmetric stretching modes of PO_2^- in the phosphodiester groups in phospholipids, whereas absorptions centered at ~1165 cm^{-1} and ~1060 cm^{-1} matched the ester C–O–C vibrations of phospholipid, cholesterol ester and fatty acid.[3-5]

A dendrographic analysis of all FTIR measurements at sites of atheromas (employing d-value distances measure, Ward's algorithm, together with the distribution of the z-values, graphics not shown) suggested that the FTIR spectra of atherosclerotic aorta could be grouped into four categories (type I –IV) (Fig. 2a to 2d; heavy lines), based on their spectral similarity. To determine if the observed spectral patterns of reflected light could be linked to particular pathologic features, we conducted additional FTIR measurements on several model systems; including atherogenic lipoproteins, phospholipid particles, activated macrophages, late-stage or

disintegrating foam cells, and smooth muscle cells (Fig. 3). These biologic materials and cell lines are characteristic of atheromatous disease and its progression.[12, 13] Although the exact hydrogen-bond environments of molecules in these model systems are different from those in actual tissue samples, they do mirror the different compositions of pathologic material found within atherosclerotic plaques, and form the basis of our subsequent comparative analyses (Fig. 2a to 2d; light lines).

Using the data from the model systems above we found that the type-I spectrum (Fig. 2a, heavy lines), based on its spectral shape and the sharply defined high absorptions (at ~2925, ~2852, and ~1745 ~1465, ~1375, ~1240, ~1165, ~1090, and ~1060 cm^{-1}), indicates the dominant presence of lipoproteins and phospholipids (Fig. 3a; light line). For the type-II spectrum (Fig. 2b; heavy line), its overall spectral shape indicates the presence of foam cells (Fig. 2b; light line) in addition to lipoprotein and phospholipid; a characteristic of VPs. The type-III spectrum exhibits a fine structure of a triplet of peaks at ~1275, ~1235, and ~1205 cm^{-1}, and a doublet of peaks at ~1083 and ~ 1033 cm^{-1} (Fig. 2c; heavy line), which are indicative of type-I collagen [3, 5] and possibly smooth muscle cells (Fig. 2c; light line). Smooth muscle cells in VPs have been reported to orchestrate the assembly of type-I collagen.[14] Finally, the type-IV spectrum (Fig. 2d; heavy line) exhibits spectral features in the region >1400 cm^{-1} typical of the spectral character of disintegrating foam cells (Fig. 2d; light line), especially spectral region between 1200 and 1000 cm^{-1} in which there was a conspicuous absence of the PO_2^- group absorption peaks that are characteristic of nucleic acids and various oligo- and polysaccharides; most of which were probably degraded during apoptotic cell death.

We then repeated FTIR measurements on the diseased aortas from three additional ApoE (-/-) mice (three month old adult females) and two wild-type controls, and found similar results.

These data support the hypothesis that the pathologic components within atheromas cause both the reflection of infrared light and the characteristic absorption patterns observed in experimental atherosclerosis. Further studies are required to determine if these new findings can be translated to the diseased vessels of other animal models or humans where the dimensions of atherosclerotic plaques and their position beneath the endothelial cell layer are much larger than that seen in the diseased aortas of ApoE (-/-) mice.

Figure Legends

Fig. 1 Examples of infrared reflectivity from aortic atheromas. Typical intensity profiles of (**a**) the incoming synchrotron infrared beam, (**b**) reflected signals from atheromas, and (**c**) from non-atherosclerotic sites. (**d**) The corresponding reflection-absorption spectra of (**b**) shared spectral characteristics that were consistent with known excitation effects by infrared photons on atoms of molecules that are known to characterize atherosclerotic plaques. Each plot shows the averaged spectrum (black trace) ± 1.0 standard deviation (gray trace); n = 26.

Fig. 2 Comparing spectral variations with the pathologic components of atheromas. (**a**) Spectral variations in the type-I spectrum of atheromas (heavy line) can be explained (see text) by the two-component model spectrum of mixed AL+PP (light line). (**b**) Spectral variations in the type-II spectrum of atheromas (heavy line) can be explained (see text) by the three-component model spectrum of mixed AL+PP+FC (light line). (**c**) Spectral variations in the type-III spectrum of atheromas (heavy line) can be explained (see text) by the four-component model spectrum of AL+PP+FC+SMC (light line). **Insert,** a close-up comparison of the type-III spectrum of atheromas (heavy line) with the composite spectrum of AL+PP+FC+SMC (light line). The triplet of peaks in 1300-1200 cm^{-1} and the doublet of peaks in 1100-1000 cm^{-1} closely match the typical spectral pattern of type-I collagen (see text). (**d**) Spectral variations in the type-IV spectrum of

atheromas (heavy line) can be explained (see text) by the spectrum of disintegrating foam cells (light line). Legend: R, reflectance; AL, atherogenic lipoproteins; PP, phospholipid particles; AM, activated macrophages; FC, late-stage foam cells; and SMC, smooth muscle cells. Spectral markers of key functional groups in the solid-state atherosclerotic components are highlighted.

Fig. 3 Examples of mid-infrared FTIR reflection spectra obtained from the individual pathologic components associated with atherosclerosis. Photomicrographs and reflection-absorption FTIR spectra of atherogenic lipoprotein (AL), phospholipid particles (PP), activated macrophages (AM), late-stage foam cells (FC), smooth muscle cells (SMC), and disintegrating foam cells (DFC) are displayed. Each spectrum is an average of at least twenty different samples. Purified chicken egg yolk and bacterial lipopolysaccharides (from *Salmonella minnesota*) were purchased from Sigma-Aldrich (MO, USA). J774.1 murine macrophage cells were obtained from the American Tissue Culture Collection (ATCC). Thin films of egg yolk (model atherogenic lipoprotein[15]) were prepared from the powder of the purified egg yolk which was suspended in distilled sterile water and dried under a stream of nitrogen gas. We recorded the spectra of extracellular phospholipid particles and smooth muscle cells that were isolated from transverse micro-dissections of frozen ApoE(-/-) mouse tissues. To obtain spectra of macrophage and macrophage-derived foam cells, we activated mouse macrophages (J774.1) in culture with bacterial molecules, and obtained foam cells by feeding the activated macrophages cholesterol-containing liposomes. The spectra of each stage of foam cell evolution were measured at different time points: 24 hours (early-stage foam cells), 48 hours (mature-stage foam cells), and 72 hours (late-stage foam cells). To obtain the spectra of disintegrating foam cells, we fed activated macrophages excess cholesterol-containing liposomes for 96 hours. Scale bars for

photomicrographs: PP, 5 µm; AM, FC, DFC, 10 µm; and SMC, 15 µm. Spectral markers of key functional groups are highlighted.

Acknowledgements

Supported in part by the U.S. Department of Energy, Office of Science and Office of Biological and Environmental Research, Medical Science Division under Contract Nos. DE-AC03-76SF00098 and DE-AC02-05CH11231.

References

1. M. Gossl, D. Versari, H. Hildebrandt, D. Mannheim, M. L. Olson, L. O. Lerman, and A. Lerman, "Vulnerable plaque: Detection and management," Medical Clinics of North America **91**(4), 573-601 (2007).
2. J. M. Gentner, E. Wentrup-Byrne, P. J. Walker, and M. D. Walsh, "Comparison of fresh and post-mortem human arterial tissue: An analysis using FT-IR microspectroscopy and chemometrics," Cellular and Molecular Biology **44**(1), 251-259 (1998).
3. K. Z. Liu, I. M. C. Dixon, and H. H. Mantsch, "Distribution of collagen deposition in cardiomyopathic hamster hearts determined by infrared microscopy," Cardiovascular Pathology **8**(1), 41-47 (1999).
4. A. Becker, M. Epple, K. M. Muller, and I. Schmitz, "A comparative study of clinically well-characterized human atherosclerotic plaques with histological, chemical, and ultrastructural methods," Journal of Inorganic Biochemistry **98**(12), 2032-2038 (2004).
5. D. L. Wetzel, G. R. Post, and R. A. Lodder, "Synchrotron infrared micro spectroscopic analysis of collagens I, III, and elastin on the shoulders of human thin-cap fibroatheromas," Vibrational Spectroscopy **38**(1-2), 53-59 (2005).
6. H.-Y. N. Holman and M. C. Martin, "Synchrotron radiation infrared spectromicroscopy: a non-invasive molecular probe for biogeochemical processes.," in *Advances in Agronomy*, D. Sparks, ed. (Elsevier, New York, 2006), pp. 79-127.
7. M. Claybourn, "Mid-infrared External Reflection Spectroscopy," in *Handbook of Vibrational Spectroscopy*, J. M. Chalmers and P. R. Griffiths, eds. (Wiley Interscience, London, 2002), pp. 969-981.
8. V. P. Maltsev, A. V. Chernyshev, K. A. Semyanov, and E. Soini, "Absolute real-time determination of size and refractive index of individual microspheres," Measurement Science & Technology **8**(9), 1023-1027 (1997).
9. B. J. Tarasevich, C. C. Chusuei, and D. L. Allara, "Nucleation and growth of calcium phosphate from physiological solutions onto self-assembled templates by a solution-

formed nucleus mechanism," Journal of Physical Chemistry B **107**(38), 10367-10377 (2003).
10. L. J. J. Dirckx, L. C. Kuypers, and W. F. Decraemer, "Refractive index of tissue measured with conflocal microscopy," Journal of Biomedical Optics **10**(4), - (2005).
11. H. D. Downing and D. Williams, "Optical-Constants of Water in Infrared," Journal of Geophysical Research **80**(12), 1656-1661 (1975).
12. P. Libby and P. Theroux, "Pathophysiology of coronary artery disease," Circulation **111**(25), 3481-3488 (2005).
13. R. Virmani, S. Malik, A. Burke, K. Skorija, N. Wong, F. Kolodgie, and J. Narula, "Vulnerable plaque pathology for imagers," Circulation **114**(18), 385-385 (2006).
14. M. M. Kockx, G. Y. De Meyer, N. Buyssens, M. W. M. Knaapen, H. Bult, and A. G. Herman, "Cell composition, replication, and apoptosis in atherosclerotic plaques after 6 months of cholesterol withdrawal," Circulation Research **83**(4), 378-387 (1998).
15. D. Kritchevsky, "Dietary-Protein, Cholesterol and Atherosclerosis - a Review of the Early History," Journal of Nutrition **125**(3), S589-S593 (1995).

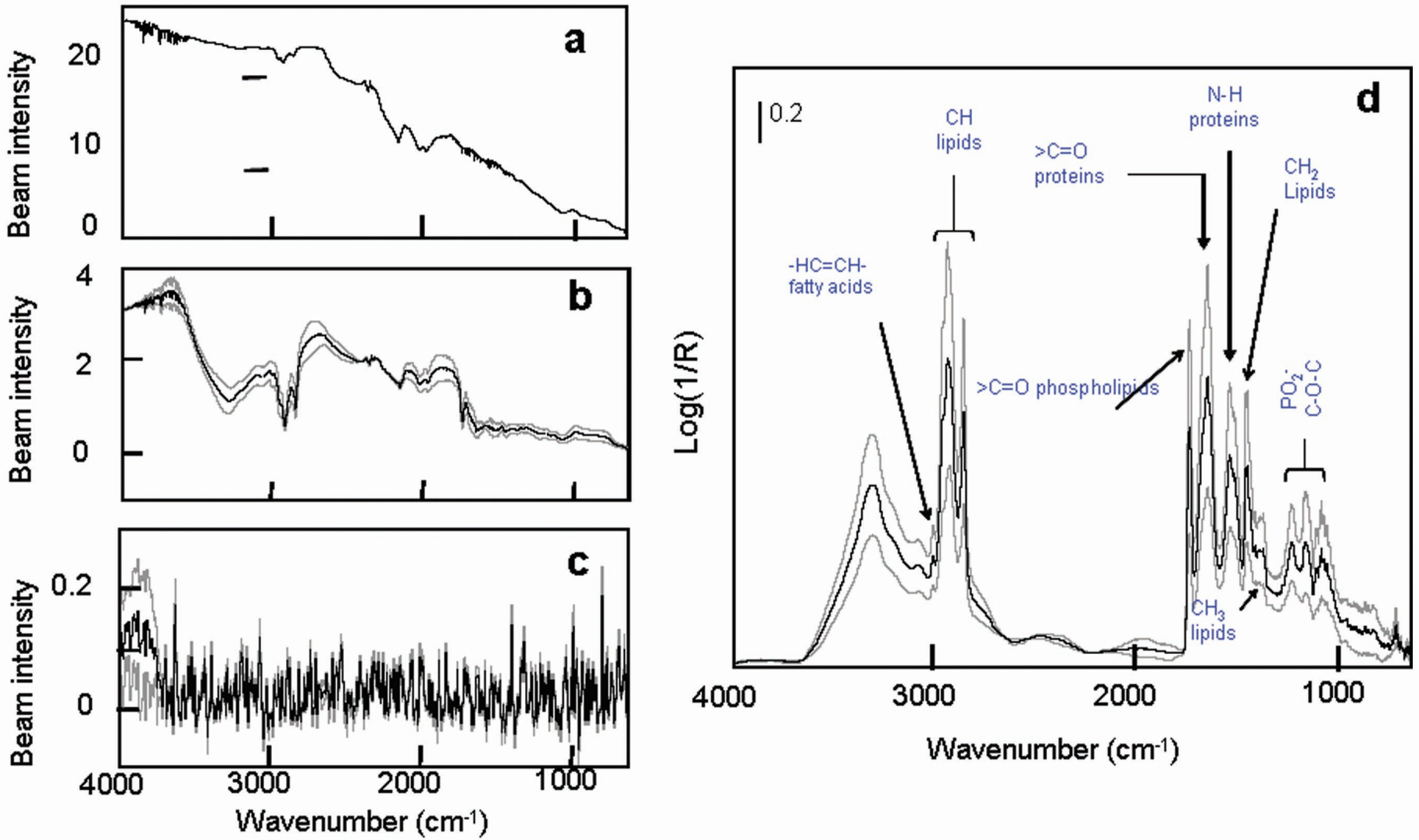
a
b
c
d
Beam intensity
20
10
0
4
2
0
0.2
0
4000
3000
2000
1000
Wavenumber (cm-1)
0.2
Log(1/R)
CH
lipids
>C=O
proteins
N-H
proteins
CH2
Lipids
-HC=CH-
fatty acids
>C=O phospholipids
PO2-
C-O-C
CH3
lipids

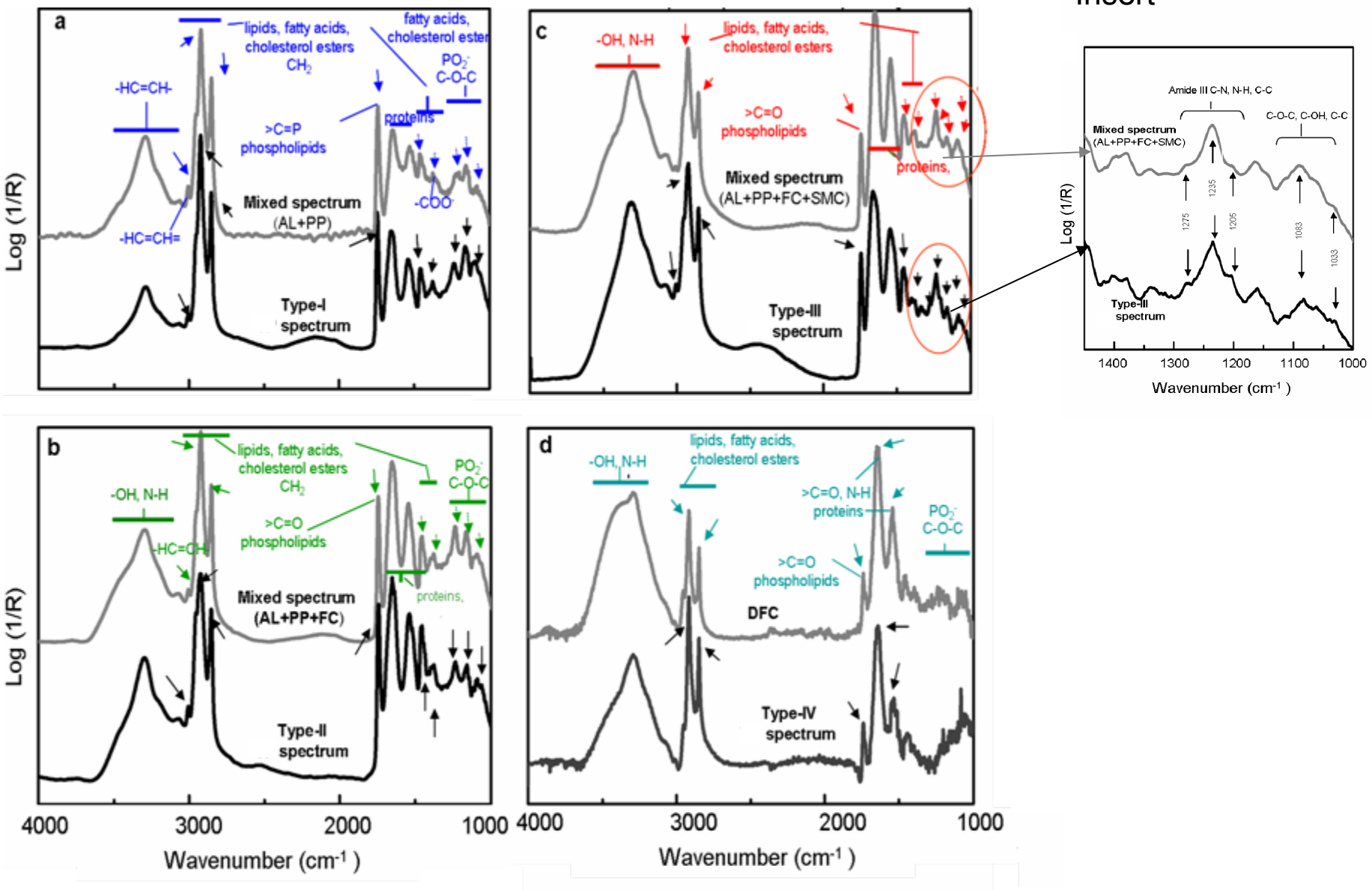
Insert
a
lipids, fatty acids, cholesterol esters CH2
fatty acids, cholesterol ester
PO2- C-O-C
-HC=CH-
>C=P phospholipids
proteins
-COO-
-HC=CH=
Mixed spectrum (AL+PP)
Type-I spectrum
c
-OH, N-H
lipids, fatty acids, cholesterol esters
>C=O phospholipids
proteins,
Mixed spectrum (AL+PP+FC+SMC)
Type-III spectrum
Amide III C-N, N-H, C-C
C-O-C, C-OH, C-C
Mixed spectrum (AL+PP+FC+SMC)
1275
1235
1205
1083
1033
Type-III spectrum
Log (1/R)
1400
1300
1200
1100
1000
Wavenumber (cm-1)
b
lipids, fatty acids, cholesterol esters CH2
PO2- C-O-C
-OH, N-H
-HC=CH-
>C=O phospholipids
proteins,
Mixed spectrum (AL+PP+FC)
Type-II spectrum
d
-OH, N-H
lipids, fatty acids, cholesterol esters
>C=O, N-H proteins
PO2- C-O-C
>C=O phospholipids
DFC
Type-IV spectrum
Log (1/R)
4000
3000
2000
1000
Wavenumber (cm-1)

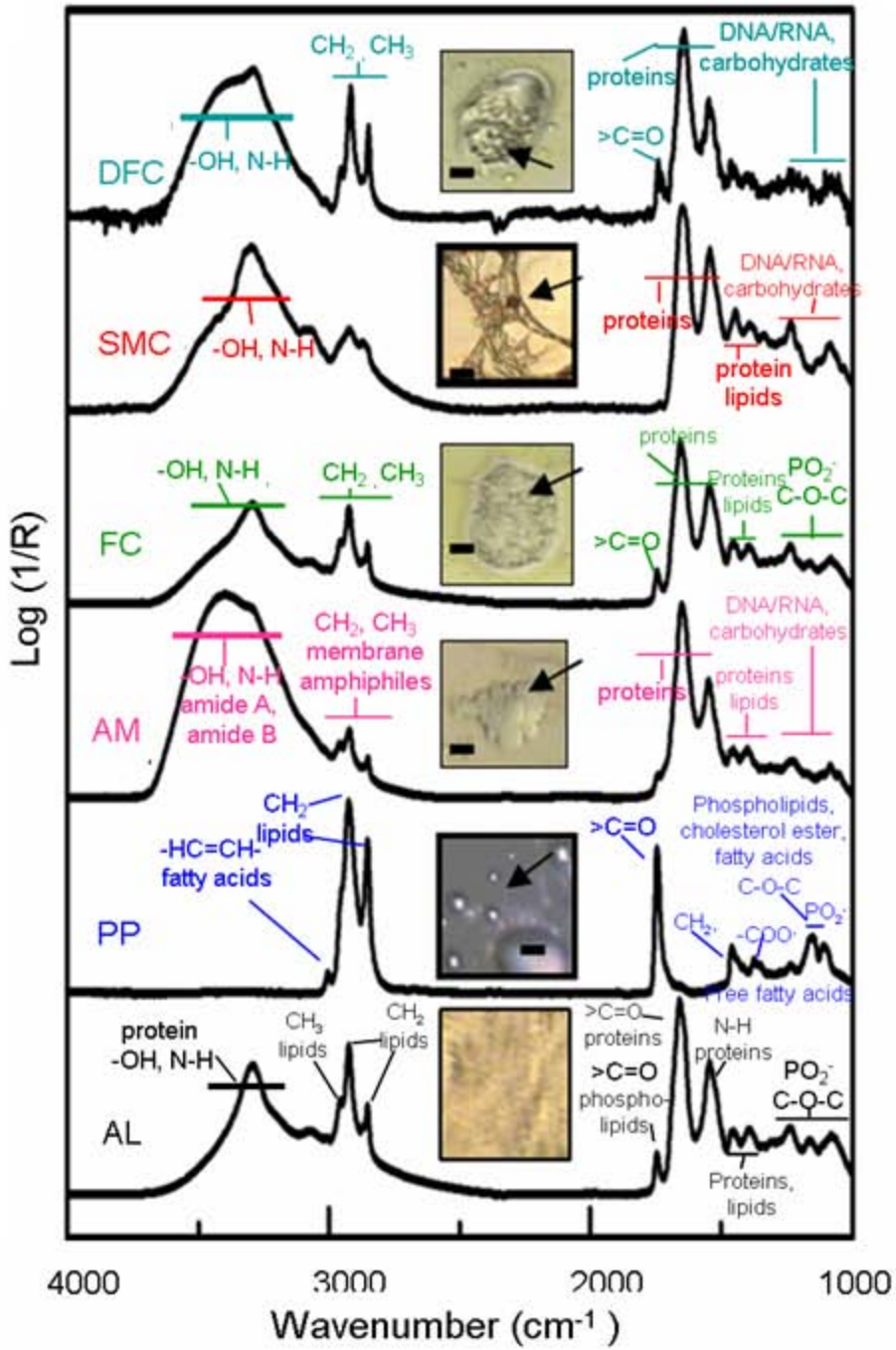
DFC
SMC
FC
AM
PP
AL
Log (1/R)
Wavenumber (cm-1)
4000
3000
2000
1000
CH2, CH3
-OH, N-H
proteins
DNA/RNA, carbohydrates
>C=O
protein lipids
-OH, N-H, amide A, amide B
CH2, CH3 membrane amphiphiles
proteins lipids
CH2 lipids
-HC=CH- fatty acids
Phospholipids, cholesterol ester, fatty acids
C-O-C
PO2-
CH2
-COO-
Free fatty acids
protein -OH, N-H
CH3 lipids
CH2 lipids
>C=O proteins
>C=O phospho-lipids
N-H proteins
Proteins, lipids